

Reactive Power Sharing in Islanded Microgrids Using Adaptive Voltage Droop Control

Hisham Mahmood, *Member, IEEE*, Dennis Michaelson, *Member, IEEE*, and Jin Jiang, *Senior Member, IEEE*

Abstract—In this paper, a strategy that employs an adaptive voltage droop control to achieve accurate reactive power sharing is investigated. Instead of controlling the output voltage of the inverter directly, the voltage droop slope is tuned to compensate for the mismatch in the voltage drops across feeders by using communication links. If the communication channel is disrupted, the controller will operate with the last tuned droop coefficient, which is shown to still outperform the controller with the initial fixed droop coefficient. Also, the net control action of the adaptive droop terms is demonstrated to have a negligible effect on the microgrid bus voltage. Since communication is not used within the tuning control loop, the strategy is inherently immune to delays in communication links. A small-signal model of the proposed controller is presented, and the effectiveness of the proposed strategy is demonstrated on a 1.2 kVA prototype microgrid.

Index Terms—Distributed generation (DG), droop control, microgrid control, reactive power sharing.

I. INTRODUCTION

ISLANDED operation can be considered as one of the most attractive features of a microgrid, since it ensures service continuity in the event of a grid interruption [1]. When islanded, distributed generation (DG) units must be able to cooperatively regulate the voltage and frequency, and maintain the generation/load power balance within the microgrid. Accordingly, droop control concepts have been widely adopted in [2]–[4] to provide decentralized power sharing control without relying on communications. Moreover, communications can be used, in addition to droop control, as a noncritical element in a higher control layer known as secondary control to enhance the performance of the islanded microgrid without reducing the system reliability [5]–[11].

Although the frequency droop technique can be used to achieve accurate real power sharing, voltage droop control commonly results in poor reactive power sharing [12]. This is due to the mismatch in the voltage drops across the DG unit feeders, which is induced by the mismatch in the feeder impedances and/or the differences in the power ratings of the

units [13]. Therefore, the problem of reactive power sharing has been investigated extensively in [14]–[28].

The mismatch in the output impedances of the closed-loop voltage controller of the DG units is the focus in [14]–[16]. With a properly designed controller, these impedances are negligible around the operating frequency range in comparison to the feeder impedances. However, the mismatch in the feeder physical impedances, including the transformers, cables, and interface reactors, is not considered [17], which can have a significant effect on the accuracy of the reactive power sharing.

The technique developed in [18] requires the microgrid to operate in the grid connected mode prior to islanding in order to estimate the physical feeder impedances. The accuracy of this strategy has been validated for units with different virtual impedances and identical feeder impedances.

A control strategy is proposed for microgrids with resistive impedances in [19]. It is assumed that the inverter output impedance can be dominated by a resistive virtual impedance, while ignoring the feeder physical impedance which may include cable impedance, transformer impedance, and/or the interface reactor. However, in practice, the feeders may have both prominent inductive and resistive components [18], that have different values for each unit. The proposed strategy in [20] results in reducing but not eliminating the sharing error. For example, the sharing error is reduced from 6.47% to 3.1% for a slight mismatch in the feeder impedances of $0.02 + j0.075 \Omega$.

Communication is used in [17] and [21]–[28] to improve the reactive power sharing accuracy. The sharing error is reduced but not eliminated in [21] (as in [20]). Also, time delays in communications (e.g., 16 ms) may reduce the reactive power sharing accuracy significantly. Control strategies proposed in [22] and [23] require instantaneous control signal interconnections between units, which might not be feasible if the DG units are located at different geographical locations.

Adaptive virtual impedances are used in [24] to achieve accurate reactive power sharing. However, the case where the DG units have different ratings is not discussed.

A strategy based on feeder impedance estimation is introduced in [25] and [26]. Feeder impedances are estimated using the voltage harmonics at the point of common coupling (PCC), assuming that the phase angle difference between the PCC voltage and the DG unit output is negligible. This assumption may not be valid for higher power levels and/or longer feeders.

Manuscript received July 8, 2014; revised October 10, 2014 and December 2, 2014; accepted January 15, 2015. This work was supported by the Natural Sciences and Engineering Research Council of Canada. Paper no. TSG-00697-2014.

The authors are with the Department of Electrical and Computer Engineering, Western University, London, ON N6A 5B9, Canada (e-mail: jijiang@eng.uwo.ca).

Color versions of one or more of the figures in this paper are available online at <http://ieeexplore.ieee.org>.

Digital Object Identifier 10.1109/TSG.2015.2399232

The power sharing strategy in [27] is divided into two stages: 1) a conventional droop control; and 2) a compensation stage. Communication is used to synchronize the start and the end of these stages. During the compensation stage, frequency droop control is used to achieve accurate sharing of the reactive power. At the same time, an integral voltage droop term is used to regulate the real power at a fixed value, which is the real power shared prior to the start of the compensation stage. The scenario in which the real power load changes during the compensation stage is not shown. In this case, the integral term still attempts to regulate the output power at a fixed value, which may impact stability.

Secondary control strategies that employ communications are investigated in [17] and [28], which can achieve accurate reactive power sharing. However, the scenario of lost communication and its effect on reactive power sharing is not considered.

In this paper, an adaptive voltage droop control is proposed to compensate for the effect of voltage drops across feeder impedances, in order to improve reactive power sharing. Tuning of the voltage droop slope is facilitated by employing communication. The contributions of this paper are reflected in the unique features that are offered by the proposed strategy, as follows.

- 1) If the communication is interrupted, the controller operates with the last tuned droop coefficient, which still outperforms the controller with the initial fixed droop coefficient.
- 2) Since communication is not used within the tuning closed loop control, the proposed strategy is inherently immune to delays in the communication links.
- 3) Furthermore, the combined action of the adaptive terms added at each DG unit results in a negligible effect on the microgrid bus voltage.
- 4) The control strategy is straightforward to implement, and does not require knowledge of the feeder parameters. Therefore, no estimation algorithm is required.

The structure of the system and the problem statement are introduced in Section II. The proposed control strategy is discussed in Section III. A small-signal model of the tuning control loop is developed in Section IV. The experimental results are presented in Section V, followed by the conclusion.

II. PROBLEM STATEMENT

A simplified diagram of an islanded microgrid, that consists of N units, is shown in Fig. 1. Note that, since the reactive power sharing problem exists only during islanded operation, only the islanded control mode is considered in this paper. Since the focus in this paper is on the fundamental real and reactive power, only linear loads are considered as in [18]–[20], and [27]. Each DG unit has the capability to exchange information with the central energy management system (EMS). With proper design of the voltage controller, the voltages measured and controlled at the output of units DG 1 to DG N are assumed to follow the references V_1^* to V_N^* , respectively. The frequency and voltage references for each

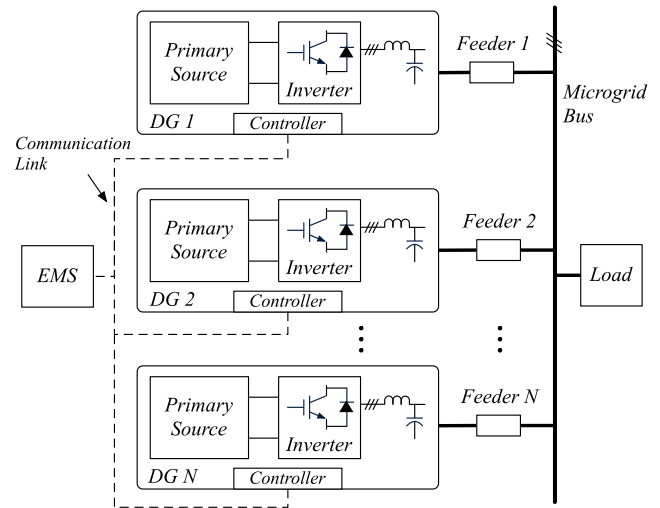


Fig. 1. Islanded microgrid structure.

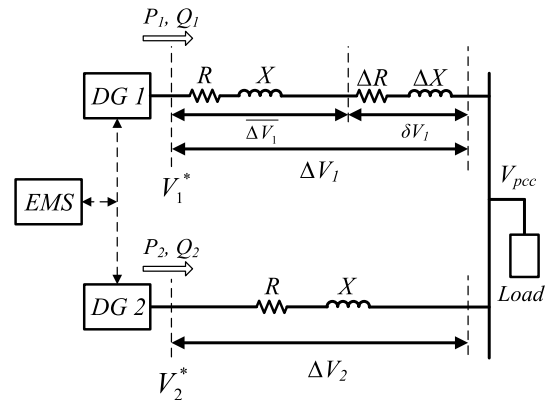


Fig. 2. Simplified diagram of the two-unit microgrid considering the feeder of DG 2 as a reference to determine the mismatch in the feeder impedances.

unit are generated using conventional droop control as follows:

$$\omega = \omega_o - mP_m \quad (1)$$

$$V^* = V_o - nQ_m \quad (2)$$

where ω and V^* are the frequency and voltage magnitude references, respectively. ω_o and V_o are the nominal system frequency and voltage, respectively. P_m and Q_m are the real and reactive powers, respectively, measured at the output of each DG unit and conditioned by first order low-pass filters. The frequency and voltage droop coefficients are denoted by m and n , respectively. The feeder impedance represents the impedances of the interface inductor and/or the isolation transformer, and the impedance of the feeder cables.

Without a loss of generality, a microgrid of two units is considered to present the problem of reactive power sharing, and to introduce the proposed control strategy as in [14], [18]–[20], and [27]. The case where both units have the same power rating is considered first to introduce the problem. In Fig. 2, the feeder of unit DG 2 is considered as a reference feeder to determine the mismatch in the feeder impedances (ΔX , ΔR), which are given by

$$\Delta R = R_1 - R_2 \quad (3)$$

$$\Delta X = X_1 - X_2 \quad (4)$$

where R_1, X_1 are the resistance and reactance of the Unit 1 feeder, and $R_2 = R, X_2 = X$ are the resistance and reactance of the Unit 2 feeder. The voltage drop across each feeder can be approximated by [18] and [27]

$$\Delta V_2 \approx \frac{XQ_2 + RP_2}{V_o} \quad (5)$$

$$\Delta V_1 \approx \frac{(X + \Delta X)Q_1 + (R + \Delta R)P_1}{V_o}. \quad (6)$$

Rearranging the terms in (6)

$$\begin{aligned} \Delta V_1 &\approx \frac{XQ_1 + RP_1}{V_o} + \frac{\Delta XQ_1 + \Delta RP_1}{V_o} \\ &= \overline{\Delta V_1} + \delta V_1. \end{aligned} \quad (7)$$

Accordingly, since $P_1 = P_2$, then $\overline{\Delta V_1} = \Delta V_2$, and δV_1 represents the mismatch in the voltage drop across the feeders. Taking the voltage at the PCC (V_{pcc}) as a reference point, the voltage drops across the system can be written as

$$V_1^* = V_{pcc} + \overline{\Delta V_1} + \delta V_1 \quad (8)$$

$$V_2^* = V_{pcc} + \Delta V_2. \quad (9)$$

The mismatch in the feeder impedances ($\Delta X, \Delta R$), and hence, in the voltage drop across the feeders (δV_1) results in errors in reactive power sharing between the units as detailed in [12], [13], [18], and [27].

However, identical feeders result in accurate sharing only if the units have the same power ratings, and correspondingly, the same droop coefficients. When the units have different power ratings, even though the feeder impedances may match, the unit supplying more power will result in a higher voltage drop across its feeder, in comparison to the unit supplying less power. The worst case may occur when the unit with the higher power rating is connected to the feeder with higher impedance, as will be shown in Section V-B.

For units with different power ratings, the feeder resistance and reactance must be made inversely proportional to the real and reactive power ratings of the respective DG unit to achieve accurate reactive power sharing [13], [25], [27]. In other words, the following should be true:

$$R_1 P_{r1} = R_2 P_{r2} \quad (10)$$

$$X_1 Q_{r1} = X_2 Q_{r2} \quad (11)$$

where P_{r1}, Q_{r1} are the real and reactive power ratings of Unit 1, and P_{r2}, Q_{r2} are those of Unit 2. Consequently, the voltage drop difference that can cause inaccurate reactive power sharing is not determined by the direct mismatch in the feeder impedances as in (3) and (4). Using the Unit 2 feeder as the reference again, R_1 and X_1 can be expressed as

$$R_1 = \frac{P_{r2}}{P_{r1}} R + \Delta R \quad (12)$$

$$X_1 = \frac{Q_{r2}}{Q_{r1}} X + \Delta X. \quad (13)$$

The conditions in (10) and (11), and stated in [13], [25], and [27], are intuitive and based on the fact that they will result in the same voltage drop across

feeders regardless of the different power ratings. To clarify this point mathematically, the voltage drops across the feeders under (12) and (13), are given by

$$\Delta V_2 \approx \frac{XQ_2 + RP_2}{V_o} \quad (14)$$

$$\Delta V_1 \approx \frac{\left(\frac{Q_{r2}}{Q_{r1}} X + \Delta X\right) Q_1 + \left(\frac{P_{r2}}{P_{r1}} R + \Delta R\right) P_1}{V_o}. \quad (15)$$

If the conditions in (10) and (11) are satisfied, i.e., $\Delta R = 0$ and $\Delta X = 0$, then (15) can be reduced to

$$\Delta V_1 \approx \frac{\left(\frac{Q_{r2}}{Q_{r1}} X\right) Q_1 + \left(\frac{P_{r2}}{P_{r1}} R\right) P_1}{V_o}. \quad (16)$$

Given the fact that real power sharing using frequency droop is always accurate, i.e., $(P_{r2}/P_{r1}) = (P_2/P_1)$, (16) can be rewritten as

$$\Delta V_1 \approx \frac{\left(\frac{Q_{r2}}{Q_{r1}} X\right) Q_1 + RP_2}{V_o}. \quad (17)$$

Examining (14) and (17)

$$\Delta V_1 = \Delta V_2 \Leftrightarrow \frac{Q_2}{Q_1} = \frac{Q_{r2}}{Q_{r1}}. \quad (18)$$

Therefore, regardless of the power ratings of different units, compensating for any mismatch in the voltage drop across feeders (δV_1) will result in accurate reactive power sharing [12], [13], [18], [27]. A control strategy to compensate for the effect of δV_1 is proposed in the following section.

III. PROPOSED CONTROL STRATEGY

Instead of directly modifying the output voltage reference, the slope of the voltage droop is tuned to compensate for the effect of mismatch in the voltage drop across the feeders. Accordingly, the tuned voltage droop can still outperform the conventional fixed droop approach, even when the communication link is interrupted, as will be shown in Section V.

Using (2), (8) can be rewritten as

$$V_o - n_1 Q_1 = V_{pcc} + \overline{\Delta V_1} + \delta V_1. \quad (19)$$

The voltage droop coefficient n_1 can be modified by utilizing an adaptive term \tilde{n}_1 as in

$$V_o - (n_1 + \tilde{n}_1) Q_1 = V_{pcc} + \overline{\Delta V_1} + \delta V_1. \quad (20)$$

If \tilde{n}_1 can be tuned at any load condition such that

$$\tilde{n}_1 Q_1 = -\delta V_1 \quad (21)$$

then (20) can be reduced to

$$V_o - n_1 Q_1 = V_{pcc} + \overline{\Delta V_1}. \quad (22)$$

Therefore, the mismatch in the voltage drop across the feeders is essentially eliminated in (22). The controller proposed to tune the voltage droop and achieve accurate reactive power sharing is shown in Fig. 3. Tuning of the voltage droop slope is facilitated by utilizing the reactive power share reference Q^* ,

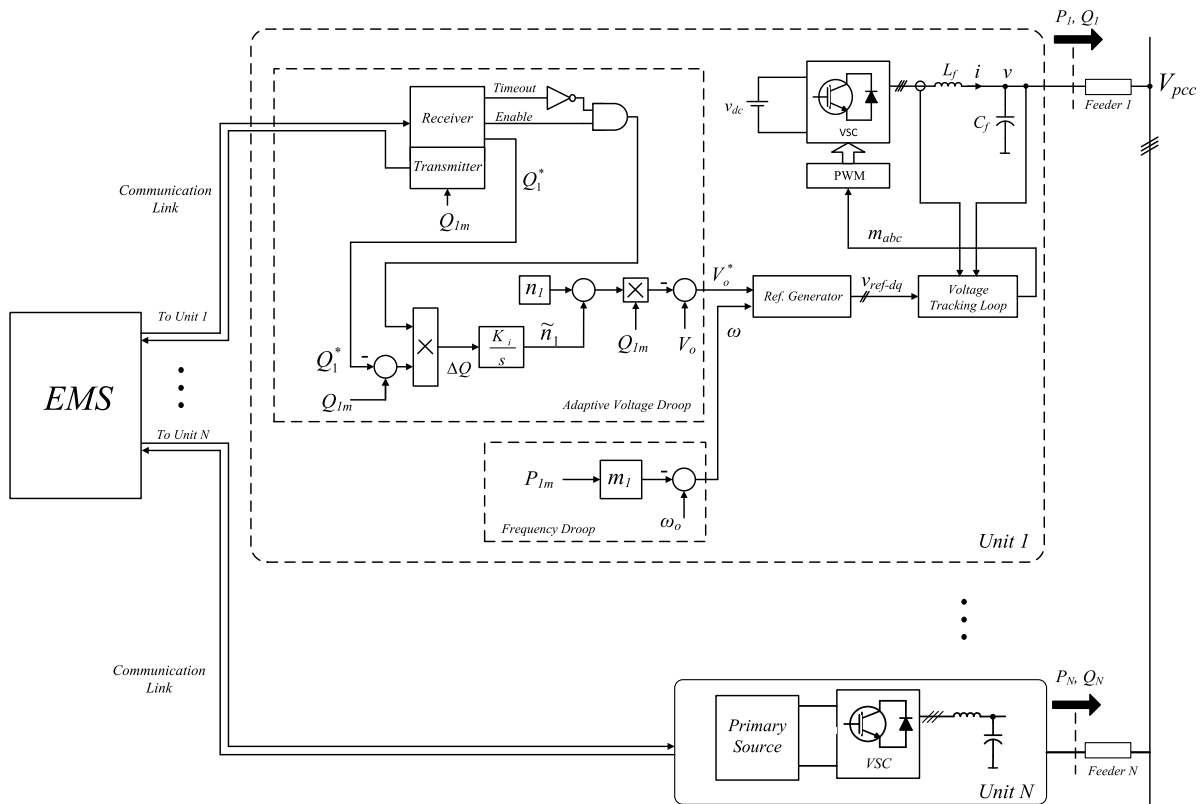


Fig. 3. Proposed adaptive droop control for a single unit.

which is made available by the EMS over a communication link. Each unit sends its measured reactive power, periodically, to the EMS which calculates the proper share for each unit based on the unit rating and the total load. Accordingly, each unit receives its share reference back from the EMS.

The reference Q_1^* is used to tune the droop coefficient \tilde{n}_1 using an integral controller that is implemented locally in the DG unit, as shown in Fig. 3. The reference Q_1^* is calculated based on the total reactive power demand in the microgrid. Therefore, even when Q_1 and Q_2 change individually during the tuning process, $Q_1 + Q_2$ remains unchanged unless the total load demand changes. In other words, the reference Q^* is only affected by the total load disturbance not by the action of the tuning loops. When the total load changes, the reference Q^* will be adjusted accordingly and the local controller starts taking action as in any supervisory control system. In other words, the tuning loop is closed locally at each DG unit, and not through communications. Since communication is not used in the local tuning control loop, the accuracy of the reactive power sharing is unaffected by any communication delays, which is not the case with the techniques in [21]–[23].

At the receiver end, a time-out function is utilized as shown in Fig. 3. When a communication time-out is detected, the binary signal “Timeout” will disable the controller ($\Delta Q = 0$). Therefore, the integrator output (\tilde{n}) will be held at the last value until the communication link is restored. In addition, when the EMS experiences a time-out in communication with any DG unit, it will stop sending the references Q^* to all the units. Consequently, the tuning process will be disabled in all

units, which will continue operating at the most recent droop slope. The signal “Enable” is used to remotely enable/disable the controller during experiments.

In general the controller shown in Fig. 3 can be implemented in all of the units of the microgrid. In this case, the effect of the added adaptive droop term (\tilde{n}) will result in a negligible effect on the voltage of the microgrid bus (load voltage). This is due to the fact that under the proposed controller, the unit with a higher voltage drop across its feeder (lower reactive power) will try to reduce the voltage droop slope, and the unit with a lower voltage drop across its feeder (higher reactive power) will try to increase the voltage droop slope. Therefore, the net effect on the bus voltage will be negligible as will be shown in Section V.

The integral controller gain K_i is chosen such that the controller dynamics are much slower than the reference update rate. For example, K_i is chosen as $0.00005 \text{ V}/(\text{s} \cdot \text{var}^2)$ (Table I), which results in a settling time of approximately 1.45 s (see Section IV), in comparison to the reference update period of 0.2 s. Therefore, the time delay in the received reference will not induce any significant control action by the time the correct updated reference is received, which is within one sampling period. A time delay of longer than the update period causes the receiver to timeout until the next updated reference is received. Note that the delay in the received Q^* is composed of both the time between the instant of a reactive power load change and the subsequent sampling instant for Q^* , and any additional delays introduced by the communication channel.

TABLE I
SYSTEM PARAMETERS

Description	Parameter	Value
Nominal Voltage (line-line)	V_o	208 V _{l-l}
Nominal Frequency	ω_o	377 rad/s
Unit 1:		
Feeder 1 Impedance	$R_1 + jX_1$	1.6 + j2.450 Ω
Frequency Droop	m_1	0.00105 rad/(s · W)
Voltage Droop	n_1	0.005 V/var
Integral Gain	K_{i-1}	0.00005 V/(s · var ²)
Unit 2:		
Feeder 2 Impedance	$R_2 + jX_2$	1.1 + j1.508 Ω
Frequency Droop - Case 1	m_2	0.00105 rad/(s · W)
Frequency Droop - Case 2	m_2	0.00210 rad/(s · W)
Voltage Droop - Case 1	n_2	0.005 V/var
Voltage Droop - Case 2	n_2	0.010 V/var
Integral Gain - Case 1	K_{i-2}	0.00005 V/(s · var ²)
Integral Gain - Case 2	K_{i-2}	0.00010 V/(s · var ²)
Total Test Load	P_L, Q_L	800 W, 900 var
Q^* Setpoint Update Rate	f_c	5 Hz
LPF Time Constant	T	0.032 s

Note that, as with the fixed droop slope, the integral gains are chosen to be inversely proportional to the power ratings of each unit, $K_{i-1}Q_1 = K_{i-2}Q_2$. In this case, the controller action results in a proportional effect on the total droop slope ($n + \tilde{n}$).

When the desired slope is obtained through the control action, the system will operate as a conventional droop controller with a droop slope of $n + \tilde{n}_o$, where \tilde{n}_o is the tuned slope, until the next load change. From (7) and (21)

$$\tilde{n}_o Q_o \approx -\frac{\Delta X Q_o + \Delta R P_o}{V_o} \quad (23)$$

where Q_o and P_o are the reactive and real power at the considered operating point, respectively. Dividing both sides of (23) by Q_o and rearranging terms

$$\tilde{n}_o \approx -\left(K_x + K_r \frac{P_o}{Q_o}\right) \quad (24)$$

where $K_x = (\Delta X/V_o)$, and $K_r = (\Delta R/V_o)$. As can be concluded from (24), the change in \tilde{n}_o depends on the change in the ratio P_o/Q_o , as well as on the mismatch in the resistive component of the feeder impedances. Therefore, the smaller the ΔR , the less sensitive the tuned controller is to changes in the ratio P_o/Q_o . Accordingly, this would result in a smaller sharing error when communication is lost. Also, the change in \tilde{n}_o is proportional to the ratio P_o/Q_o , which is uniquely related to the load power factor. Hence, the smaller the change in the power factor, the less the need for controller retuning, and the less the sharing error in the event of a communication interruption.

IV. SMALL SIGNAL STABILITY ANALYSIS

In the proposed strategy, the voltage droop coefficient is considered as the controlled variable. To gain insight into the stability of the adaptive droop control, a small-signal model

is developed. The real and reactive power flows at the output of the DG unit are given as [29]

$$P = \frac{(RV^{*2} - RV^*V_{pcc} \cos \delta + XV^*V_{pcc} \sin \delta)}{R^2 + X^2} \quad (25)$$

$$Q = \frac{(XV^{*2} - XV^*V_{pcc} \cos \delta - RV^*V_{pcc} \sin \delta)}{R^2 + X^2} \quad (26)$$

where R and X are the resistive and inductive components of the feeder impedance of the unit under consideration, δ is the power angle, and V_{pcc} is the microgrid bus voltage. The integral control in Fig. 3, and the modified voltage droop can be written as

$$\tilde{n} = \frac{1}{s} (Q_m - Q^*) \quad (27)$$

$$V^* = V_o - (n + \tilde{n}) Q_m. \quad (28)$$

Linearizing equations (25)–(28), along with the frequency droop equation in (1), around an operating point

$$\begin{aligned} \Delta P &= \left(\frac{\partial P}{\partial V^*}\right) \Delta V^* + \left(\frac{\partial P}{\partial \delta}\right) \Delta \delta \\ &= K_{pv} \Delta V^* + K_{p\delta} \Delta \delta \end{aligned} \quad (29)$$

$$\begin{aligned} \Delta Q &= \left(\frac{\partial Q}{\partial V^*}\right) \Delta V^* + \left(\frac{\partial Q}{\partial \delta}\right) \Delta \delta \\ &= K_{qv} \Delta V^* + K_{q\delta} \Delta \delta \end{aligned} \quad (30)$$

$$\Delta \tilde{n} = \frac{K_i}{s} \Delta Q_m \quad (31)$$

$$\Delta V^* = -n_o \Delta Q_m - Q_o \Delta \tilde{n} \quad (32)$$

$$\Delta \omega = -m \Delta P_m \quad (33)$$

where $n_o = n + \tilde{n}_o$. K_{pv} , $K_{p\delta}$, K_{qv} , and $K_{q\delta}$ are evaluated at the same considered operating point. Considering the first-order low-pass filter used in the measurement channel, and that $\Delta \omega = s \Delta \delta$, (33) can be written as

$$\Delta \delta = \frac{-m}{s(Ts + 1)} \Delta P = G_\delta(s) \Delta P. \quad (34)$$

Substituting for ΔP from (34) in (29)

$$\Delta \delta = \frac{K_{pv} G_\delta(s)}{1 - K_{p\delta} G_\delta(s)} \Delta V^* = G_{\delta v}(s) \Delta V^*. \quad (35)$$

Equation (35) represents the coupling between the reactive power controller and the real power/frequency droop control. Using (30)–(32) and (35), a block diagram of the system can be realized as in Fig. 4. Simplifying the block diagram, the system characteristic equation is given by

$$a_5 s^5 + a_4 s^4 + a_3 s^3 + a_2 s^2 + a_1 s + a_0 = 0 \quad (36)$$

where

$$a_5 = T^3 \quad (37)$$

$$a_4 = n_o K_{qv} T^2 + 3T^2 \quad (38)$$

$$a_3 = 2n_o K_{qv} T + 3T + K_{p\delta} m T^2 + K_i Q_o K_{qv} T^2 \quad (39)$$

$$\begin{aligned} a_2 &= -n_o m K_{q\delta} K_{pv} T + n_o m K_{qv} K_{p\delta} T + 2m K_{p\delta} T \\ &\quad + 2K_i Q_o T K_{qv} + n_o K_{qv} + 1 \end{aligned} \quad (40)$$

$$\begin{aligned} a_1 &= -m K_i Q_o K_{q\delta} K_{pv} T + m K_i Q_o K_{qv} K_{p\delta} T + K_i Q_o K_{qv} \\ &\quad - n_o m K_{q\delta} K_{pv} + n_o m K_{qv} K_{p\delta} + K_{p\delta} m \end{aligned} \quad (41)$$

$$a_0 = -m K_i Q_o K_{q\delta} K_{pv} + m K_i Q_o K_{qv} K_{p\delta}. \quad (42)$$

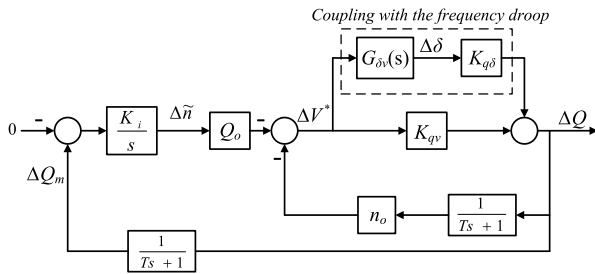


Fig. 4. Small-signal model of the droop tuning controller.

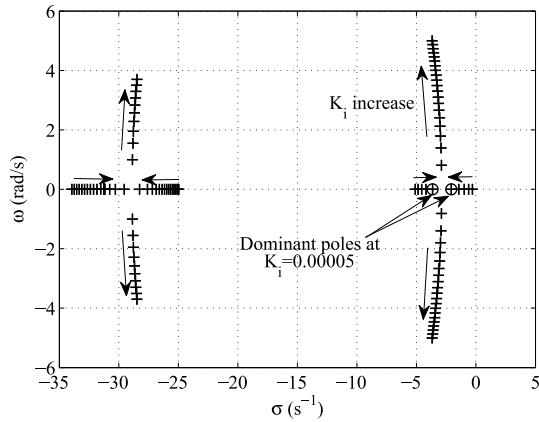
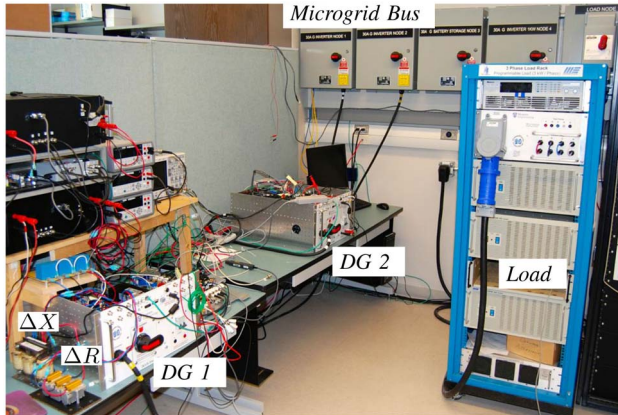
Fig. 5. Root trajectories when K_i is varied from 0.00001 to 0.00025.

Fig. 6. Experimental microgrid.

Based on (36), the pole trajectories when the integral controller gain is changed from 0.00001 to 0.00025 with a step of 0.00001, are shown in Fig. 5. Note that four poles are affected by the change in K_i , whereas the pole at $\sigma = -31.25 \text{ s}^{-1}$ is completely insensitive to K_i . As mentioned in Section III, the gain K_i is chosen as $0.00005 \text{ V}/(\text{s} \cdot \text{var}^2)$, which results, in the most dominant pole to be at $\sigma = -2.07 \text{ s}^{-1}$, as shown in Fig. 5. This is equivalent to a settling time of 1.45 s based on the 5% settling time definition.

V. EXPERIMENTAL VALIDATION

The performance of the proposed control strategy is validated on the two-unit experimental microgrid shown in Fig. 6. The parameters of the system are included in Table I.

Two cases are considered to validate the performance of the proposed strategy. In Case 1, the strategy is first validated for units with the same power rating as in [14], [18]–[20], and [27], to provide an intuitive visual measure of the sharing accuracy, since the units are expected to share both the real and the reactive power equally in this case.

In Case 2, a mismatch in both the power ratings and the feeder impedances is considered. As shown in Table I, the droop coefficients of Unit 2 are set such that it appears to have half the rating of Unit 1, i.e., $m_2 = 2m_1$ and $n_2 = 2n_1$.

The units are implemented with insulated-gate bipolar transistor-based 3-phase inverters controlled by Texas Instruments TMS320F28335 floating-point microcontrollers, and are programmed using the Simulink Embedded Coder tool-chain. The EMS is programmed in Python and run on a PC platform under Ubuntu Linux. An Ethernet network is used to connect the EMS to the units using Texas Instruments Ethernet-to-serial converters.

To evaluate the performance of the proposed controller, the following measure of the reactive sharing error is used as in [20]:

$$Q_{err-i} = \frac{Q_i - Q_i^*}{Q_i^*} 100\% \quad (43)$$

where Q_{err-i} is the sharing error for unit i , Q_i refers to the actual reactive power supplied by unit i , and Q_i^* is the desired reactive power share that each unit i should ideally supply.

A. Case 1: Units With the Same Power Rating and Different Feeder Impedances

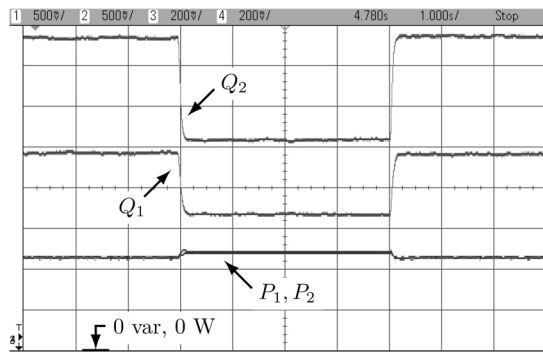
The performance of the proposed controller is validated in the following experimental scenarios.

1) *Conventional Versus Adaptive Droop*: The performance of the conventional voltage droop is shown in Fig. 7(a). The load is changed between 900 var and 809 W, and 609 var and 878 W. This represents a change of 291 var in the reactive power versus -69 W in the real power, which is selected to examine the tuning control performance under a considerable change in the ratio P/Q . From Fig. 7(a), the sharing errors are -26.7% and 26.7% for Units 1 and 2, respectively, at the higher reactive load.

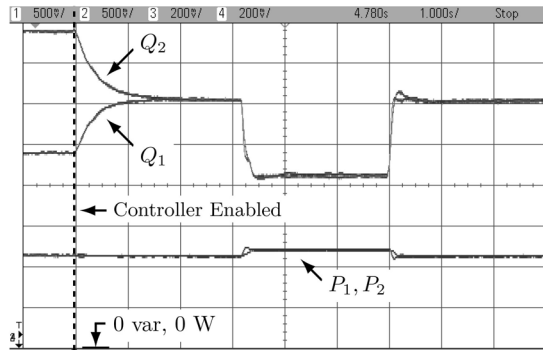
The performance of the system when the proposed controller is enabled and during a load change is shown in Fig. 7(b). As can be seen, the tuning process takes about 1.5 s, and results in accurate power sharing with tolerable transients.

2) *Performance During Communication Interruption*: The performance of the system during a communication interruption is shown in Fig. 8. In this experiment, the Ethernet cable connected to Unit 2 is physically unplugged to break the communication channel. In Fig. 8(a), the voltage drop has been tuned for the load conditions when the communication is lost as marked by the controller timeout signal. The units share the reactive power accurately until the reactive power is stepped up by 291 var, whereas the real power is decreased by 69 W. In this case, the sharing error increases to 1.47% which is still lower than the error in the conventional droop case (26.6%).

On the other hand, the system has been tuned for the higher reactive load in Fig. 8(b), and then the real power

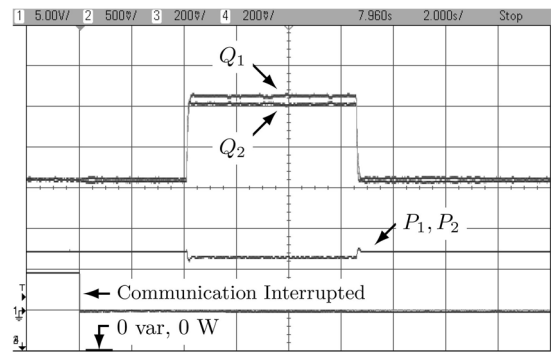


(a)

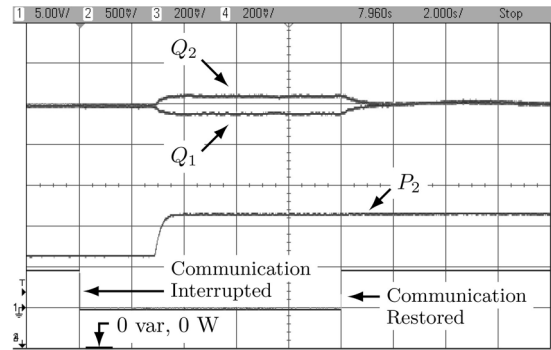


(b)

Fig. 7. Performance of the proposed controller versus the conventional voltage droop control—Case 1 (Q : 72.4 var/div, P : 181 W/div, time: 1 s/div). (a) Conventional control. (b) Proposed control strategy.



(a)



(b)

Fig. 8. Performance of the proposed controller during a communication interruption—Case 1 (Q : 72.4 var/div, P : 181 W/div, time: 2 s/div). (a) During a reactive power change. (b) During a real power change.

load is stepped up by 385 W to show the performance of the system under a considerable change in the ratio P/Q , and also in the real power. The sharing error in this case is 3.8%. Communication restoration is also shown in Fig. 8(b), when the Ethernet cable is plugged back in.

3) *Effect of Communication Time Delay*: The effect of time delays in communication is investigated by introducing a delay in the signal sent to Unit 1. In this case, the Unit 2 controller receives the reactive power reference (Q^*) and starts acting before Unit 1 does, which has more effect on the transients in comparison to the case when the delays are identical. The introduced time delay is chosen as 0.1 s, which is significant given that the reference update period is 0.2 s (see Table I). The system performance when the controller is enabled, and during a load change, is shown in Fig. 9. As shown, the time delay has little effect on the system transients. Most importantly, the time delay does not affect the sharing accuracy, unlike the method in [21], or in the techniques that require the availability of instantaneous control interconnections [22], [23]. It is worth mentioning that if the delay increases beyond the reference update period (0.2 s in this case), the controller will time out until the next reference is received, similar to the time out and restoration shown in Fig. 8(b). The time delay of 0.1 s will still be used for the rest of the experiments.

4) *Proposed Controller Effect on the Voltage of the Microgrid Bus*: To show the effect of the added adaptive droop term on the voltage of the microgrid bus (load voltage), the upper peaks of the phase-a bus voltage, zoomed to 5 V/div,

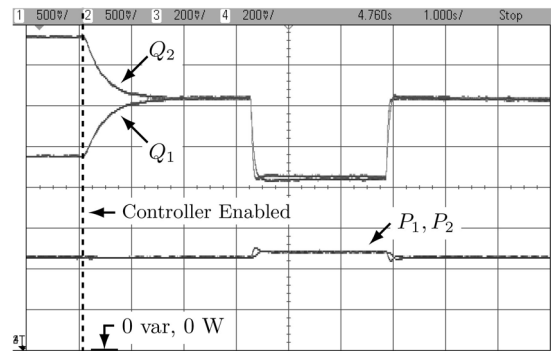


Fig. 9. Performance of the proposed controller with a communication delay—Case 1 (Q : 72.4 var/div, P : 181 W/div).

are shown in Fig. 10 to indicate the voltage amplitude when the controller is enabled. As explained in Section III, the controller has a negligible effect on the bus voltage.

B. Case 2: Units With Different Power Ratings and Different Feeder Impedances

The performance of the conventional voltage droop in this case is shown in Fig. 11. The load is changed between 736 var and 757 W, and 572 var and 830 W.

Conventional droop results in maximum sharing errors of $Q_{err-2} = 70.3\%$ at the low reactive power load, and $Q_{err-2} = 63.0\%$ at the high reactive power load. Under the low reactive power load condition, Unit 2 is supplying 324 var,

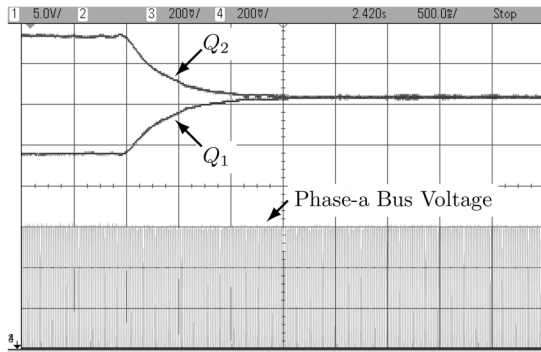


Fig. 10. Effect of the proposed controller on the voltage of the microgrid bus (load voltage) (Q : 72.4 var/div, V_{pcc} : 5 V/div, time: 0.5 s/div).

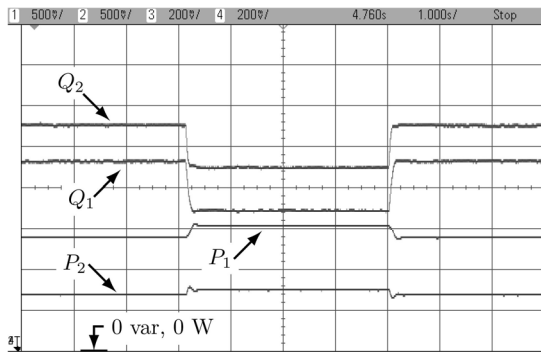


Fig. 11. Performance of the conventional voltage droop control—Case 2 (Q : 72.4 var/div, P : 181 W/div, time: 1 s/div).

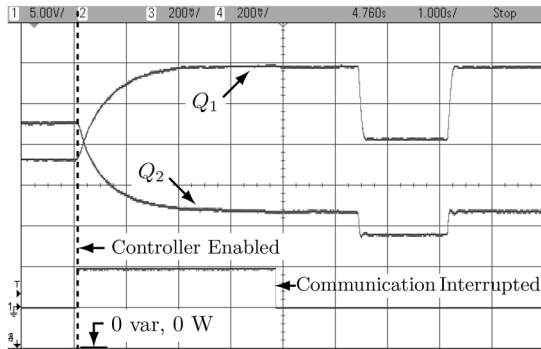


Fig. 12. Performance of the proposed controller before and after losing communications—Case 2 (Q : 72.4 var/div, P : 181 W/div, time: 1 s/div).

while Unit 1 is supplying 248 var. Ideally, Unit 2 should supply half the reactive power share of Unit 1.

The performance of the proposed controller is shown in Fig. 12. It is shown that after activating the controller, Unit 2 supplies half the reactive power share of Unit 1, 190 versus 380 var, respectively. Also, the performance of the controller after a communication disruption and a load change is shown in Fig. 12. The sharing errors under this condition are calculated as -2.7% and 5.4% , in comparison to 63.0% and 70.3% when using conventional droop control.

The performance of the proposed control strategy, measured in terms of the sharing error Q_{err} , is summarized in Table II for selected operating points.

TABLE II
REACTIVE POWER SHARING ERROR FOR
SELECTED OPERATING POINTS

Case	Conventional Droop $Q_{err-1,2}$	Proposed	
		Comm. available $Q_{err-1,2}$	Comm. Interrupted $Q_{err-1,2}$
Case 1	-26.0%, 26.0%	0.0, 0.0%	1.47%, -1.47%
Case 2	-34.8%, 70.3%	0.0, 0.0%	-2.7%, 5.4%

VI. CONCLUSION

In this paper, a control strategy to improve reactive power sharing in an islanded microgrid is developed and validated experimentally. It is shown that communications can facilitate tuning the voltage droop coefficient to compensate for the effect of the mismatch in the feeder voltage drops on the reactive power sharing. A small-signal model has been developed and the stability of the additional control loop has been analyzed. Experimental results show that the reactive power sharing using the proposed strategy is unaffected by time delays in the communication channels. Even when the communication is interrupted, the proposed control strategy can still outperform the conventional droop control. Finally, it is shown that the added voltage droop adaptive term has negligible effect on the microgrid bus voltage.

REFERENCES

- [1] M. A. Zamani, T. Sidhu, and A. Yazdani, "Investigations into the control and protection of an existing distribution network to operate as a microgrid: A case study," *IEEE Trans. Ind. Electron.*, vol. 61, no. 4, pp. 1904–1915, Apr. 2014.
- [2] J. Rocabert, A. Luna, F. Blaabjerg, and P. Rodríguez, "Control of power converters in AC microgrids," *IEEE Trans. Power Electron.*, vol. 27, no. 11, pp. 4734–4749, Nov. 2012.
- [3] I. U. Nutkani, P. C. Loh, and F. Blaabjerg, "Droop scheme with considering of operating cost," *IEEE Trans. Power Electron.*, vol. 29, no. 3, pp. 1047–1052, Mar. 2014.
- [4] D. De and V. Ramanarayanan, "Decentralized parallel operation of inverters sharing unbalanced and nonlinear loads," *IEEE Trans. Power Electron.*, vol. 25, no. 12, pp. 3015–3025, Dec. 2010.
- [5] J. M. Guerrero, M. Chandorkar, T.-L. Lee, and P. C. Loh, "Advanced control architecture for intelligent microgrids—Part I: Decentralized and hierarchical control," *IEEE Trans. Power Electron.*, vol. 60, no. 4, pp. 1254–1262, Apr. 2013.
- [6] J. M. Guerrero, J. C. Vasquez, J. Matas, L. G. de Vicuña, and M. Castilla, "Hierarchical control of droop-controlled AC and DC microgrids—A general approach towards standardization," *IEEE Trans. Ind. Electron.*, vol. 58, no. 1, pp. 158–172, Jan. 2011.
- [7] M. N. Marwali, J.-W. Jung, and A. Keyhani, "Control of distributed generation systems—Part II: Load sharing control," *IEEE Trans. Power Electron.*, vol. 19, no. 6, pp. 1551–1561, Nov. 2004.
- [8] J. C. Vasquez, J. M. Guerrero, M. Savaghebi, J. Eloy-Garcia, and R. Teodorescu, "Modeling, analysis, and design of stationary-reference-frame droop-controlled parallel three-phase voltage source inverters," *IEEE Trans. Ind. Electron.*, vol. 60, no. 4, pp. 1271–1280, Apr. 2013.
- [9] M. Savaghebi, A. Jalilian, J. C. Vasquez, and J. M. Guerrero, "Secondary control scheme for voltage unbalanced compensation in an islanded droop-controlled microgrid," *IEEE Trans. Smart Grid*, vol. 3, no. 2, pp. 797–807, Jun. 2012.
- [10] M. Savaghebi, A. Jalilian, J. C. Vasquez, and J. M. Guerrero, "Secondary control scheme for voltage quality enhancement in microgrids," *IEEE Trans. Smart Grid*, vol. 3, no. 4, pp. 1893–1902, Dec. 2012.
- [11] M. A. Abusara, J. M. Guerrero, and S. M. Sharkh, "Line-interactive UPS for microgrids," *IEEE Trans. Ind. Electron.*, vol. 61, no. 3, pp. 1292–1300, Mar. 2014.

- [12] T. L. Vandoorn, J. C. Vasquez, J. D. Kooning, J. M. Guerrero, and L. Vandevelde, "Microgrids: Hierarchical control and an overview of the control and reserve management strategies," *IEEE Ind. Electron. Mag.*, vol. 7, no. 4, pp. 42–55, Dec. 2013.
- [13] J. Kim, J. M. Guerrero, P. Rodriguez, R. Teodorescu, and K. Nam, "Mode adaptive droop control with virtual output impedances for an inverter-based flexible AC microgrid," *IEEE Trans. Power Electron.*, vol. 26, no. 3, pp. 689–701, Mar. 2011.
- [14] W. Yao, M. Chen, J. Matas, J. M. Guerrero, and Z.-M. Qian, "Design and analysis of the droop control method for parallel inverters considering the impact of the complex impedance on the power sharing," *IEEE Trans. Ind. Electron.*, vol. 58, no. 2, pp. 576–588, Feb. 2011.
- [15] J. M. Guerrero, J. Matas, L. G. de Vicuña, M. Castilla, and J. Miret, "Decentralized control for parallel operation of distributed generation inverters using resistive impedance," *IEEE Trans. Ind. Electron.*, vol. 54, no. 2, pp. 994–1004, Apr. 2007.
- [16] J. M. Guerrero, L. G. de Vicuña, J. Matas, M. Castilla, and J. Miret, "Output impedance design of parallel-connected UPS inverters with wireless load-sharing control," *IEEE Trans. Ind. Electron.*, vol. 52, no. 4, pp. 1126–1135, Aug. 2005.
- [17] A. Micallef, M. Apap, C. Spiteri-Staines, J. Guerrero, and J. Vasquez, "Reactive power sharing and voltage harmonic distortion compensation of droop controlled single phase islanded microgrids," *IEEE Trans. Smart Grid*, vol. 5, no. 3, pp. 1149–1158, May 2014.
- [18] Y. W. Li and C.-N. Kao, "An accurate power control strategy for power-electronics-interfaced distributed generation units operating in a low-voltage multibus microgrid," *IEEE Trans. Power Electron.*, vol. 24, no. 12, pp. 2977–2988, Dec. 2009.
- [19] Q.-C. Zhong, "Robust droop controller for accurate proportional load sharing among inverters operated in parallel," *IEEE Trans. Ind. Electron.*, vol. 60, no. 4, pp. 1281–1290, Apr. 2013.
- [20] C.-T. Lee, C.-C. Chu, and P.-T. Cheng, "A new droop control method for the autonomous operation of distributed energy resources interface converters," *IEEE Trans. Power Electron.*, vol. 28, no. 4, pp. 1980–1993, Apr. 2013.
- [21] Y. Zhang and H. Ma, "Theoretical and experimental investigation of networked control for parallel operation of inverters," *IEEE Trans. Ind. Electron.*, vol. 59, no. 4, pp. 1961–1970, Apr. 2012.
- [22] X. Yu, A. M. Khambadkone, H. Wang, and S. T. S. Terence, "Control of parallel-connected power converters for low-voltage microgrid—Part I: A hybrid control architecture," *IEEE Trans. Power Electron.*, vol. 25, no. 12, pp. 2962–2970, Dec. 2010.
- [23] A. M. Roslan, K. H. Ahmed, S. J. Finney, and B. W. Williams, "Improved instantaneous average current-sharing control scheme for parallel-connected inverter considering line impedance impact in microgrid networks," *IEEE Trans. Power Electron.*, vol. 26, no. 3, pp. 702–716, Mar. 2011.
- [24] H. Mahmood, D. Michaelson, and J. Jiang, "Accurate reactive power sharing in an islanded microgrid using adaptive virtual impedances," *IEEE Trans. Power Electron.*, vol. 30, no. 3, pp. 1605–1617, Oct. 2014.
- [25] J. He, Y. W. Li, J. M. Guerrero, J. C. Vasquez, and F. Blaabjerg, "An islanded microgrid reactive power sharing scheme enhanced by programmed virtual impedances," in *Proc. IEEE Int. Symp. Power Electron. Distrib. Gener. Syst.*, Aalborg, Denmark, 2012, pp. 229–235.
- [26] J. He, Y. W. Li, J. M. Guerrero, F. Blaabjerg, and J. C. Vasquez, "An islanding microgrid power sharing approach using enhanced virtual impedance control scheme," *IEEE Trans. Power Electron.*, vol. 28, no. 11, pp. 5272–5282, Nov. 2013.
- [27] J. He and Y. W. Li, "An enhanced microgrid load demand sharing strategy," *IEEE Trans. Power Electron.*, vol. 27, no. 9, pp. 3984–3995, Sep. 2012.
- [28] Q. Shafiee, J. M. Guerrero, and J. C. Vasquez, "Distributed secondary control for islanded microgrids—A novel approach," *IEEE Trans. Power Electron.*, vol. 29, no. 2, pp. 1018–1031, Feb. 2014.
- [29] E. A. A. Coelho, P. C. Cortizo, and P. F. D. Garcia, "Small signal stability for single phase inverter connected to a stiff AC system," in *Proc. IEEE 34th Ind. Appl. Conf.*, Phoenix, AZ, USA, 1999, pp. 2180–2187.



Hisham Mahmood (S'10–M'15) received the M.E.Sc. degree in control engineering from Lakehead University, Thunder Bay, ON, Canada, and the Ph.D. degree in electrical engineering from the University of Western Ontario, London, ON, Canada, in 2008 and 2014, respectively.

He is currently a Post-Doctoral Fellow with the Department of Electrical and Computer Engineering, University of Western Ontario. His current research interests include modeling and control of switching power converters, distributed generation, renewable

energy interface, microgrids, and power quality.



Dennis Michaelson (M'12) received the B.A.Sc. degree in automation engineering from Simon Fraser University, Burnaby, BC, Canada, in 1993. He is currently pursuing the Ph.D. degree from the Department of Electrical and Computer Engineering, Western University, London, ON, Canada.

He was the Vice-President of Engineering at EK3 Technologies, Inc., London, where he led a team developing networked embedded systems for multimedia applications. His current research interests include control of energy storage in microgrids,

power electronic converters, mobile robotics, and embedded real-time systems.



Jin Jiang (S'85–M'87–SM'94) received the Ph.D. degree from the University of New Brunswick, Fredericton, NB, Canada in 1989.

Since 1991, he has been with the Department of Electrical and Computer Engineering, Western University, London, ON, Canada, where he is currently a Senior Industrial Research Chair Professor. He is also with the International Atomic Energy Agency, Wien, Austria, working on modern control and instrumentation for nuclear power plants. His current research interests include fault-tolerant control of safety-critical systems, advanced control of electrical power plants, and power systems involving renewable energy resources.

Dr. Jiang is a Fellow of the Canadian Academy of Engineering. He is a Member of the International Electrotechnical Commission 45A Subcommittee to develop industrial standards on instrumentation and control for nuclear facilities.